

# Dual polarization kinetic inductance detectors for large imaging cameras at millimeter wave bands

E. Artal\*<sup>a</sup>, B. Aja<sup>a</sup>, L. de la Fuente<sup>a</sup>, J.P. Pascual<sup>a</sup>, E. Villa<sup>a,b</sup>,  
M.C. de Ory<sup>b</sup>, D. Rodriguez<sup>b</sup>, V. Rollano<sup>b</sup>, M.T. Magaz<sup>b</sup>, A. Gomez<sup>b</sup>,  
D. Granados<sup>c</sup>

<sup>a</sup>Departamento de Ingeniería de Comunicaciones, Universidad de Cantabria, Santander, Spain

<sup>b</sup>Centro de Astrobiología (CSIC-INTA), Torrejón de Ardoz, Madrid, Spain

<sup>c</sup>IMDEA-Nanociencia, Cantoblanco, Madrid, Spain

## ABSTRACT

This work deals with the development of superconducting Kinetic Inductance Detectors (KIDs) for highly sensitive radio astronomy receivers within W-band (75 to 110 GHz). A bilayer based on superconducting titanium/aluminum (Ti/Al) thin films has been used for assessing its absorption performance in this frequency band at millikelvin temperature. A lumped-element inductor based on a 4th order Hilbert structure is designed to absorb the incoming radiation in two orthogonal linear polarizations. The development of a large-format camera prototype is presented. On one hand, ambient temperature quasi-optical characterization demonstrates a suitable absorption for both polarizations within the W-band. On the other hand, dark cryogenic characterization confirms the successful operation of the multiplexed KID devices providing high-quality factors and an operation yield of 97%. These results confirm these developments to be used in future polarimeter receivers.

**Keywords:** Kinetic Inductance Detectors, millimeter-wave radio astronomy, polarimeter

## 1. INTRODUCTION

In the last few years, low temperature detectors based on superconducting materials have demonstrated significant results in terms of sensitivity to reach new scientific milestones in applications such as radio astronomy. In this sense, the characterization of the polarization of the Cosmic Microwave Background (CMB) radiation is a crucial observational tool that enhances our understanding of the early Universe. Kinetic Inductance Detectors (KIDs) are a type of superconducting detectors that have shown good performance within millimeter-wave bands as well as the ability to be fabricated into large arrays, making them well-suited for detecting polarization patterns of the CMB. Another significant advantage of using KIDs is their frequency-domain multiplexing readout system, in which multiple detectors can be read simultaneously in a single transmission line. These benefits make KIDs an excellent choice for large-scale, high-resolution experiments, aimed at studying the polarization of CMB. Concretely, lumped-element KIDs (LEKIDs) use a lumped element design where the components of the resonator (inductor and capacitor) are spatially separated and the inductor acts directly as the effective optical absorber.

Several ground-based experiments have demonstrated the maturity of LEKIDs, making them competitive with other technologies for next-generation millimeter and sub-millimeter wave experiments [1, 2]. Significant advantages have been made in developing dual-polarization designs based on Hilbert fractal structures, aiming to improve optical efficiency [3, 4]. This option involves duplicating the number of arrays and integrating an external polarizer [5] which not only enhances optical efficiency, but also mitigates sensitivity to misalignment issues. On the other hand, dual-polarization-sensitive LEKIDs allow simultaneous measurement of both horizontal and vertical polarizations within one spatial pixel. In this context, several demonstrators have been presented in sub-mm bands [6] and also for ground-based CMB polarimetry [7-10].

Design, fabrication and experimental tests of a Hilbert-based LEKID structure operating in the W-band, based on a bilayer of titanium/aluminum (Ti/Al) superconducting thin film, are described in this paper. It is organized as follows. Sect. 2 deals with the mm-wave quasi-optical coupling design and its absorption characterization in the W-band at

ambient temperature. Sect. 3 presents a large-format polarimetric camera demonstrator including its preliminary dark cryogenic characterization. Finally, the conclusions are presented in Sect. 4.

## 2. W-BAND LEKIDS DESIGN

LEKIDs are a kind of pair-breaking detectors based on superconducting materials with a broad range of applications in the mm and submm range, where they have provided extraordinary performance as compared with the traditional semiconductor detectors. However, the use of superconducting materials able to absorb at a specific frequency band is limited by the energy required to break Cooper pairs, which is related to the superconducting gap, and thus, to the critical temperature of the superconductor. In order to diminish the cut-off frequency down to W-band, a bilayer of titanium and aluminum is required, pushing the  $T_c$  below 1 K [11]. In particular, a 35 nm thick Ti/Al bilayer film with  $782 \pm 2$  mK critical temperature is employed with 1.27 Ohm/sq and 3 Ohm/sq sheet resistances at 1 K and at 300 K, respectively.

In LEKIDs, the inductor acts as the absorbing area, and, therefore, its geometry needs to be carefully designed to absorb the two orthogonal components of an incoming radiation within W-band. The presented design is able to detect the radiation of two linearly polarized orthogonal waves by means of a 4th order Hilbert structure, over a high-resistivity silicon substrate ( $\epsilon_r=11.9$ ). The structure impedance at W-band is matched to the free space impedance (377 Ohm) through a silicon thickness ended in a back-short, in order to maximize the absorption. Moreover, it depends on the sheet resistance of the superconducting material and its filling factor over the absorbing area [12]. Therefore, for a LEKID design sensitive to two orthogonal polarizations, a constant filling factor as well as symmetric structure in both cases are needed. Finally, the impedances that the LEKID have for both polarizations must be similar to be properly matched simultaneously.

### 2.1 Hilbert LEKIDs

The design presented describes a proposal to obtain a proper absorption for orthogonal polarizations, based on a fractal structure over a single substrate layer. The structure is optimized with HFSS ANSYS 3D electromagnetic simulator using Floquet ports, exciting the structure with two orthogonal plane waves. With this simulation a planar-periodic structure is reduced to a single unit cell defining primary and secondary boundaries.

To improve the optical coupling, a design based on a Hilbert geometry is presented. The topology provides a constant filling factor over the whole detection area, guaranteeing a homogeneous optical coupling. It has a symmetrical configuration which enables it to absorb the same power in both polarizations with a common backshort [12].

The inductor is configured in a 4th order Hilbert geometry, covering an absorbing area of 3.3 mm x 3.3 mm with a strip width of 3  $\mu\text{m}$ , and short straight sections of 220  $\mu\text{m}$ . The detector is designed on a high-resistive silicon substrate ( $\epsilon_r=11.9$ ) which enables it to be matched to free-space impedance with a back-shortened  $0.25\lambda$  thick silicon ( $\lambda$  at 90 GHz) which corresponds to a Si thickness of 240  $\mu\text{m}$ . The inductor, together with an interdigital capacitor to configure the resonant circuit, is coupled to a transmission line for readout purposes. The designed LEKID structure is shown in Figure 1 (a). The simulation of this design using the resistive sheet at cryogenic temperature ( $R_s=1.27$  Ohm/sq) and the required Si substrate thickness, shown in Figure 1 (a), predicts a maximum absorption at 90 GHz for orthogonal polarizations of an incident plane wave.

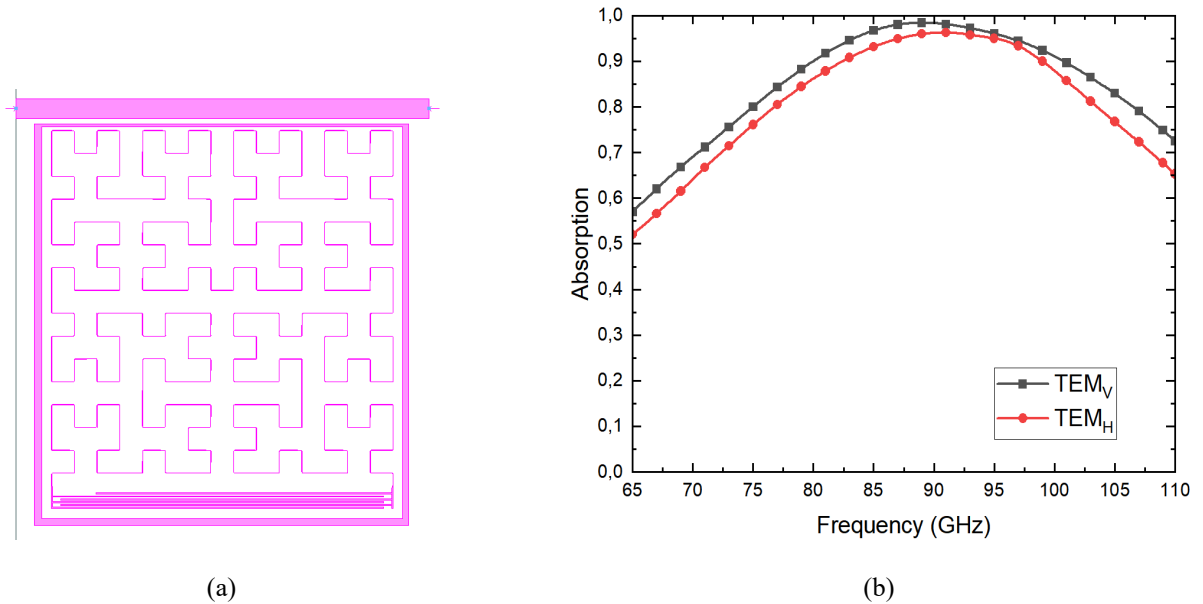


Figure 1. Hilbert LEKID design. (a) Artistic view of one resonator used for simulations (size: 3.4 mm x 3.8 mm). (b) Predicted Ti/Al LEKIDs array absorption at cryogenic temperature ( $R_s = 1.27$  Ohm/sq).

A prototype array is manufactured to confirm the quasi-optical design and its absorption within the W-band at ambient temperature. A sample wafer of 40 mm x 40 mm is manufactured including an array without readout lines, in which the LEKIDs structure is periodically located along the horizontal and vertical axis.

In order to evaluate the matching of the LEKID structures in the W-band, the reflection coefficient is characterized in a quasi-optical measurement test bench based on a 4f topology. The free-space test system, shown in Figure 2, uses a set of two rectangular horn antennas, two collimating dielectric lenses, and a vector network analyzer [13]. The LEKID absorption is characterized, as  $1 - |S_{11}|^2$ , through a TRL (Thru-Reflect-Load) calibration.

Figure 3 shows the measured absorption for the two orthogonal incident waves with linear polarization. The obtained simulation results are also shown for comparison purposes, which have been adapted to the ambient temperature sheet resistance ( $R_s = 3$  Ohm/sq), which is higher than under cryogenic temperature ( $R_s = 1.27$  Ohm/sq). The increase in the sheet resistance produces a slightly different impedance and lower return loss regarding the cryogenic simulation. Moreover, a frequency shift to lower values of the absorption maximum is obtained due to the fact that the sample wafers are manufactured on a silicon substrate slightly thicker than the design value.

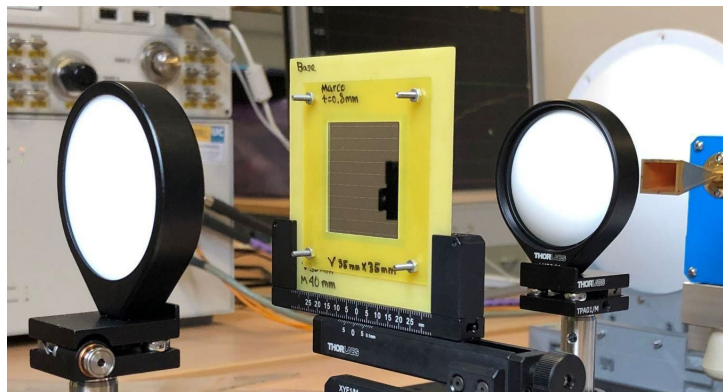


Figure 2. W-band quasi-optical system (4f topology).

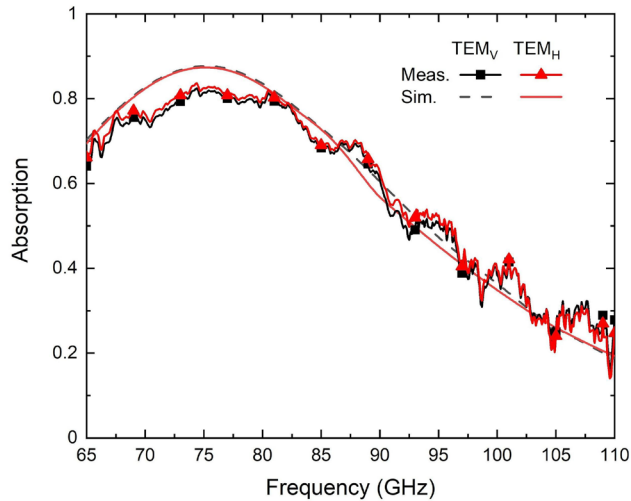


Figure 3. Hilbert Ti/Al LEKIDs array absorption at ambient temperature ( $R_s = 3 \text{ Ohm/sq}$ ).

### 3. LARGE-FORMAT ARRAY DESIGN

A prototype of a large-format polarimetric camera with 288 LEKIDs is designed, fabricated and tested in a 4-inch silicon wafer (see Figure 4). Sonnet microwave simulator is used for the low frequency design, including resonant frequency and coupling quality factor. Details on the nanofabrication process can be found in [11]. An important aspect for creating a pixel camera with LEKIDs is the distribution of resonant frequencies in the available readout bandwidth, as well as the position of adjacent pixels to avoid crosstalk between them.

Two different read-out microstrip lines are configured to implement 144 LEKIDs in each one [14], using a frequency step of 3 MHz for the LEKID resonant frequencies. Their allocation is chosen to ensure minimum crosstalk between them, and neighbor LEKIDs resonant frequencies are separated a minimum of three times the frequency step.

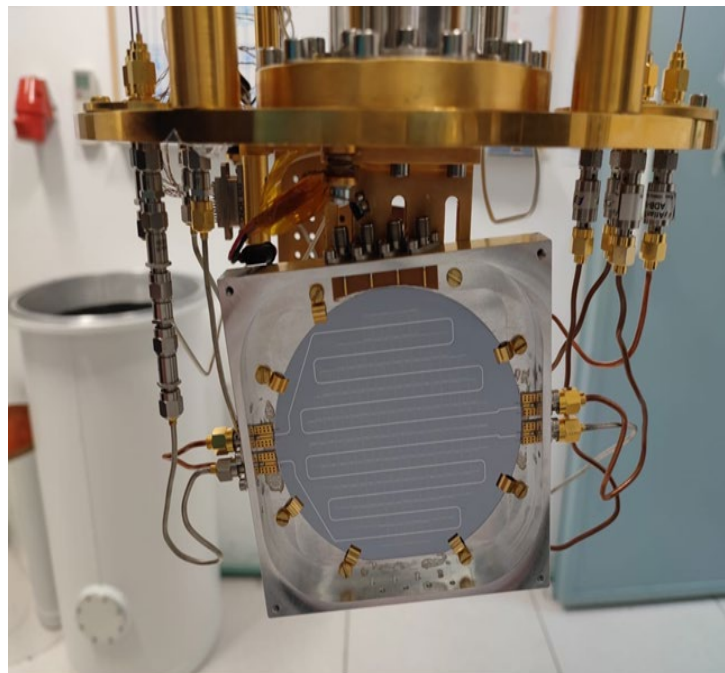


Figure 4. Large-format array demonstrator based on 288 LEKIDs with Hilbert geometry.

The response of the fabricated camera is obtained through their darkness characterization at 10 mK, in terms of its resonant frequencies and quality factors of the resonators. The experimental set-up uses a dilution refrigerator to reach subKelvin temperatures using the cryogenic harness shown in Figure 5 (a). The transmission characterization of the resonators is made with a readout system assembled in a single module shown in Figure 5 (b) [13]. This system enables two measurement set-ups: test using the vector network analyzer in the range from 40 MHz to 2.6 GHz or I/Q demodulation from 500 MHz to 2.6 GHz.

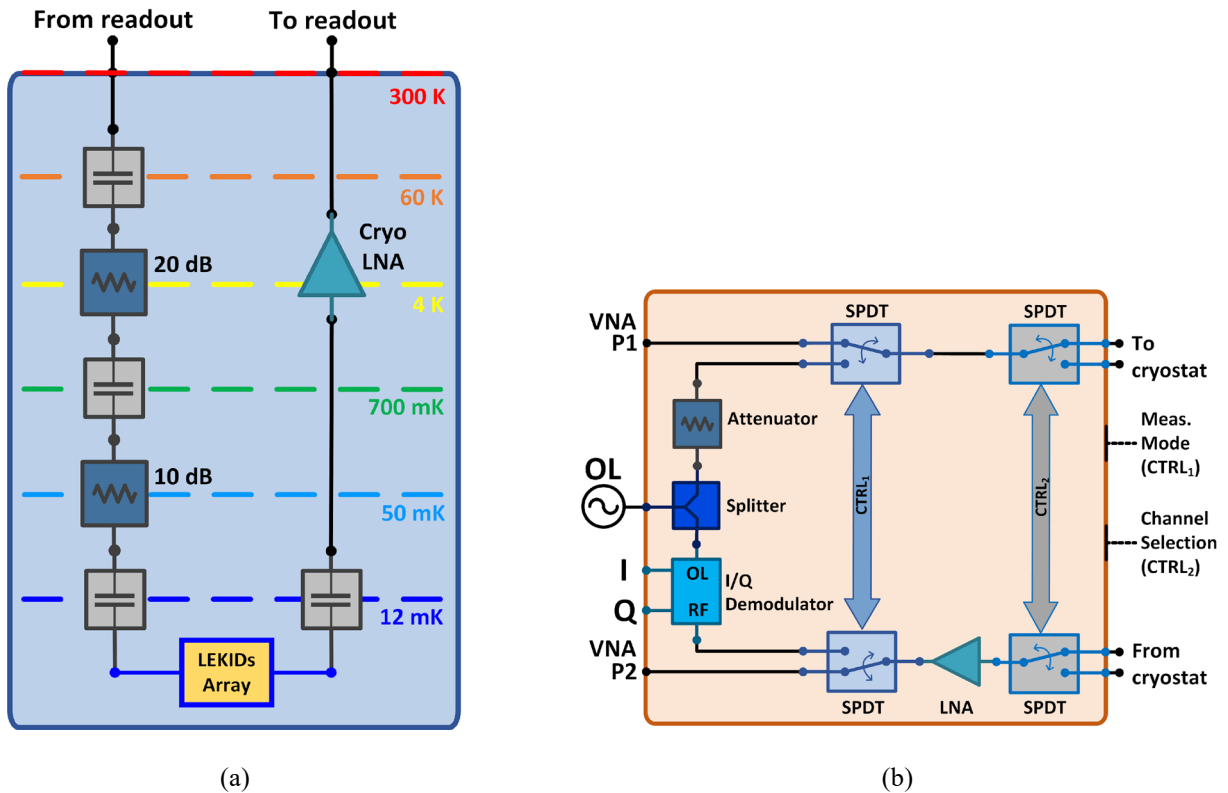


Figure 5. System set-up for cryogenic characterization. (a) Dilution cryostat harness; (b) Dual function readout system

Figure 6 depicts the measured results for one of the read-out lines of the wafer at 10 mK and -100 dBm. Figure 6 (a) shows the transmission coefficient  $S_{21}$  where each minimum corresponds to a single KID. 140 pixels out of 144 are successfully identified, providing a yield over 97%. The quality factors, in terms of the coupled  $Q_c$ , internal  $Q_i$  and loaded  $Q$ , are obtained following the fitting process explained in [15]. Measured results are shown Figure 6 (b), and the values for  $Q_c$  are around the design goal of the order of  $10^5$ .

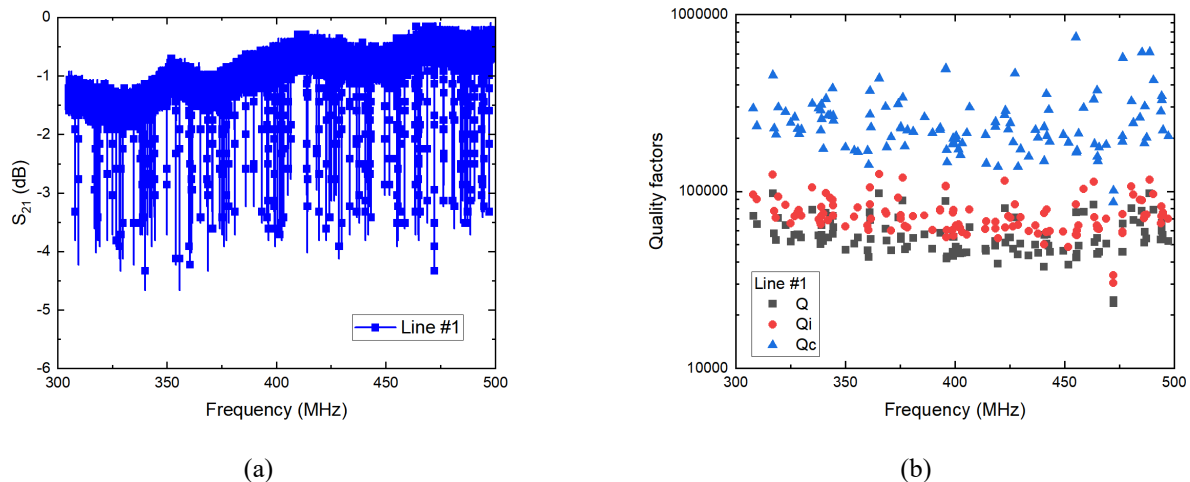


Figure 6. Cryogenic characterization at 10 mK. (a) Measured transmission coefficient; (b) Measured quality factors for all the resonant frequencies.

#### 4. CONCLUSIONS

In this work, we present the design of a large-format array based on superconducting Ti/Al lumped-element kinetic inductance detectors for the W-band. LEKIDs based on a Hilbert fractal topology are fabricated and characterized for dual polarization detection. Room temperature quasi-optical characterization shows a proper absorption at W-band for both polarizations. A large array demonstrator with hundreds of pixels is developed for future astronomical experiments. Cryogenic temperature characterization demonstrates coupled quality factors greater than  $10^5$  and a 97% yield.

#### ACKNOWLEDGEMENTS

This work is funded by the following grants: 2023/TCN/005 (Universidad de Cantabria) by Consejería de Industria, Empleo, Innovación y Comercio, Gobierno de Cantabria, Spain; PID2022-137779OB-C43 (Universidad de Cantabria), PID2022-137779OB-C41 (CAB) and PID2022-137779OB-C42 (IMDEA-Nanociencia) by MCIN/AEI/10.13039/501100011033, “ERDF A way of making Europe”, EU “NextGenerationEU”/PRTR; RED2022-134839-T (all groups) by MCIN/AEI/10.13039/501100011033. IMDEA-Nanociencia acknowledges financial support from the ‘Severo Ochoa’ Programme for Centres of Excellence in R&D (CEX2020-001039-S) and CAB from CSIC Research Platform PTI-001 and ‘Tecnologías avanzadas para la exploración del Universo y sus componentes’ (PR47/21 TAU-CM) project funded by Com. de Madrid, by the Recovery, Transformation and Resilience Plan from the Spanish State, and by NextGenerationEU from the EU Recovery and Resilience Facility.

#### REFERENCES

- [1] A. Catalano, A. Benoit, O. Bourrion, M. Calvo, G. Coiffard, A. D’addabbo, J. Goupy, H. le Sueur, J. Macías-Pérez, and A. Monfardini, “Maturity of lumped element kinetic inductance detectors for space-borne instruments in the range between 80 and 180 GHz,” *A&A* 592, A26 (2016). <https://doi.org/10.1051/0004-6361/201527715>
- [2] S. Hailey-Dunsheath, R. M. J. Janssen, J. Glenn, C. M. Bradford, J. Perido, J. Redford and J. Zmuidzinas, “Kinetic inductance detectors for the Origins Space Telescope,” *J. Astron. Telesc. Instrum. Syst.* 7 (1), 011015 (2021). <https://doi.org/10.1117/1.JATIS.7.1.011015>
- [3] S. Shu, M. Calvo, J. Goupy, A. Catalano, A. Bideaud, A. Monfardini, S. Leclercq and E. F. C. Driessen, “Optical Response of Lumped-Element Kinetic-Inductance Detector Arrays,” *IEEE Trans. Terahertz Sci. Technol.* 8 (6), pp. 605-612 (2018). <https://doi.org/10.1109/TTHZ.2018.2873127>
- [4] L. Perotto et al., “Calibration and performance of the NIKA2 camera at the IRAM 30-m Telescope,” *A&A* 637, A71 (2020). <https://doi.org/10.1051/0004-6361/201936220>

- [5] R. Adam et al., “The NIKA2 large-field-of-view millimetre continuum camera for the 30 m IRAM telescope,” *A&A* 609, A115 (2018). <https://doi.org/10.1051/0004-6361/201731503>
- [6] J. Hubmayr, J. A. Beall, D. Becker, J. A. Brevik, H. M. Cho, G. Che, M. Devlin, B. Dober, J. Gao, N. Galitzki, G. C. Hilton, K. D. Irwin, D. Li, P. Mauskopf, D. P. Pappas, J. van Lanen and M. R. Vissers, “Dual-Polarization-Sensitive Kinetic Inductance Detectors for Balloon-borne Sub-millimeter Polarimetry,” *J. Low Temp. Phys.* 176, pp. 490-496 (2014). <https://doi.org/10.1007/s10909-014-1160-2>
- [7] H. McCarrick, G. Jones, B. R. Johnson, M. H. Abitbol, P. A. R. Ade, S. Bryan, P. Day, T. Essinger-Hileman, D. Flanigan, H. G. Leduc, M. Limon, P. Mauskopf, A. Miller and C. Tucker, “Design and performance of dual-polarization lumped-element kinetic inductance detectors for millimeter-wave polarimetry,” *A&A* 610, A45 (2018). <https://doi.org/10.1051/0004-6361/201732044>
- [8] A. Catalano, J. Goupy, H. le Sueur, A. Benoit, O. Bourrion, M. Calvo, A. D’addabbo, L. Dumoulin, F. Levy-Bertrand, J. Macías-Pérez, S. Marnieros, N. Ponthieu and A. Monfardini, “Bi-layer kinetic inductance detectors for space observations between 80–120 GHz,” *A&A* 580, A15 (2015). <https://doi.org/10.1051/0004-6361/201526206>
- [9] A. Paiella, P. de Bernardis, F. Cacciotti, A. Coppolecchia, S. Masi, E. Barbavara, E. S. Battistelli, E. Carretti, F. Columbro, A. Cruciani, G. D’Alessandro, M. de Petris, F. Govoni, G. Isopi, L. Lamagna, P. Marongiu, L. Mele, E. Molinari, M. Murgia, A. Navarrini, A. Orlati, G. Pettinari, F. Piacentini, T. Pisanu, S. Poppi, G. Presta and F. Radiconi, “MISTRAL and its KIDS,” *J. Low Temp. Phys.* 209, pp. 889-898 (2022). <https://doi.org/10.1007/s10909-022-02848-z>
- [10] B. Aja, L. de la Fuente, A. Fernandez, Juan P. Pascual, E. Artal, M. C. de Ory, M. T. Magaz, D. Granados, J. Martin-Pintado, A. Gomez, “Bi-Layer Kinetic Inductance Detectors for W-Band,” 2020 IEEE/MTT-S International Microwave Symposium (IMS) (2020). <https://doi.org/10.1109/IMS30576.2020.9223828>
- [11] M. C. de Ory, D. Rodriguez, E. Villa, L. de la Fuente, B. Aja, V. Rollano, M. T. Magaz, J. P. Pascual, D. Granados, E. Artal and Alicia Gomez, “Optimized Cross-Polarized LEKIDs for W-Band Using Sawtooth Inductors,” *IEEE Trans. Microw. Theory Techn.* 72 (1), pp. 648-658 (2024). <https://doi.org/10.1109/TMTT.2023.3334816>
- [12] M. Rösch, “Development of lumped element kinetic inductance detectors for mm-wave astronomy at the IRAM 30 m telescope,” Ph.D. dissertation, Dept. Elektrotechnik Informationstechnik, Karlsruher Instituts Technologie (KIT), Karlsruhe, Germany (2014). [10.5445/KSP/1000036607](https://doi.org/10.5445/KSP/1000036607)
- [13] B. Aja, M. C. de Ory, L. de la Fuente, E. Artal, J. P. Pascual, M. T. Magaz, D. Granados and A. Gomez, “Analysis and Performance of Lumped-Element Kinetic Inductance Detectors for W-Band,” *IEEE Trans. Microw. Theory Techn.* 69 (1), pp. 578-589 (2021). <https://doi.org/10.1109/TMTT.2020.3038777>
- [14] E. Villa, M. C. de Ory, D. Rodriguez, L. de la Fuente, B. Aja, J. P. Pascual, D. Granados, E. Artal, A. Gomez, “Large-format Array of Kinetic Inductance Detectors at W-band,” *URSI 2023, XXXVIII Simposio Nacional de la Unión Científica Internacional de Radio, Spain* (2023)
- [15] S. Probst, F. B. Song, P. A. Bushev, A. V. Ustinov and M. Weides, “Efficient and robust analysis of complex scattering data under noise in microwave resonators,” *Rev. Sci. Instrum.* 86 (2), 024706 (2015). <https://doi.org/10.1063/1.4907935>